High-resolution Map of Somatic Periprostatic Nerves

Fairleigh Reeves, Shane Battye, James F. Borin, Niall M. Corcoran, and Anthony J. Costello

OBJECTIVE To generate a high-resolution map of periprostatic somatic nerves. Periprostatic nerves are at risk of injury during radical prostatectomy; this study aimed to establish the location of somatic nerves with respect to the prostate and the neurovascular bundle.

MATERIALS AND METHODS Hemiprostates from patients in whom a wide local excision was performed were evaluated. Representative sections from the base, midzone, and apex of the prostate were stained with Masson's trichrome and antineuronal nitric oxide synthase antibodies, to identify myelinated and parasympathetic nerves, respectively. Somatic nerves were identified as neuronal nitric oxide synthase negative myelinated nerves. Stained slides were scanned (40× objective) for digital analysis. Location of nerves was described with reference to 6 equal sectors per hemiprostate.

RESULTS Somatic nerves account for almost 5% of all nerve fibers in the periprostatic tissue. This study found a mean somatic nerve count of 5.83, 5.25, and 3.67 at the level of the prostate base, midzone, and apex, respectively. These nerves are most frequently located either anteriorly or in the region of the neurovascular bundle (posterolateral).

CONCLUSION Somatic nerves in the periprostatic region are at risk of injury during radical prostatectomy. Further research is required to clarify their functional relevance. UROLOGY 97: 160–165, 2016. © 2016 Published by Elsevier Inc.

Radical prostatectomy (RP) provides excellent oncological control for clinically localized prostate cancer,[1] but despite its efficacy, RP is still associated with significant morbidity for some men. Erectile dysfunction is reported in 10% to 46% of men at 12 months following RP.[2] Similarly, urinary incontinence affects 4% to 31% (no pad definition) of men at 12 months following robot-assisted RP.[3]

A detailed understanding of the periprostatic anatomy is essential for optimal functional outcomes. Awareness of the anatomy of the neurovascular bundle (NVB) and its cavernosal nerves led to the development of nerve-sparing surgery, which is strongly associated with improved potency outcomes.[2] In contrast, the pathophysiology of postprostatectomy urinary incontinence (PPI) is likely multifactorial. Whereas rhabdosphincter (RS) dysfunction has been implicated in the vast majority of cases,[4,5] the precise mechanism underlying sphincter impairment is uncertain. In particular, the neuroanatomy of urinary continence is controversial. Although most studies agree that the striated RS receives somatic innervation from the pudendal nerve,[6-9] some studies have described a separate intrapelvic supply to the RS.[7,10-12] However, these intrapelvic branches are not consistently reported and their precise course, including their relationship to the prostate and NVB, is not clear.

In a preliminary study, we undertook gross anatomical dissection of fresh cadavers to investigate the innervation of the male urethral RS (unpublished data). Evaluation of 3 adult male hemipelves demonstrated consistent supply to the RS from multiple fine branches of the perineal branch of the pudendal nerve. In these specimens, we could not confirm the presence of any intrapelvic supply to the RS. In particular, there were no early intrapelvic branches of the pudendal nerve identified. Nor were any infralevator branches of the pudendal nerve found to pierce the levator ani muscle to re-enter the pelvis on the way to the RS. However, we could not exclude the presence of nonpudendal intrapelvic somatic nerves running with the NVB. Although no branches of the NVB were seen to clearly terminate in the RS, the presence of small somatic nerves that travel with the NVB to supply the RS could not be excluded.

Due to the complex neural networks of the pelvis, the presence of fascia, and the fine caliber of these nerves, histological evaluation may be preferable in this setting as it

Financial Disclosure: *The authors declare that they have no relevant financial interests.*

From the Departments of Urology and Surgery, University of Melbourne, The Royal Melbourne Hospital, Australia; the TissuPath Pty Ltd, Mount Waverley, Australia; the Department of Urology, New York University, New York, NY; and the Australian Prostate Cancer Centre, Epworth Hospital, Australia

Address correspondence to: Fairleigh Reeves, Department of Urology, The Royal Melbourne Hospital, Level 3 Centre, Grattan St, Parkville, Vic. 3050, Australia. E-mail: fairleighr@gmail.com

Submitted: June 26, 2016, accepted (with revisions): August 1, 2016

http://dx.doi.org/10.1016/j.urology.2016.08.027
0090-4295

allows microscopic evaluation. Most histological studies investigating periprostatic neuroanatomy have however focused on autonomic nerve distribution due to their important role in erectile function,[13,14] somewhat neglecting somatic fiber distribution. Given that nerve-sparing prostatectomy is associated with improved early continence recovery,[15] we sought to finely map the anatomy of periprostatic nerves to establish if any somatic nerves, which may be destined for the RS, travel with the NVB and therefore may be at risk during RP.

The primary aim of this study was to establish at which level (base, midzone, or apex), if at all, somatic nerve fibers (potentially destined for the RS) travel with the autonomic NVB. That is, we aimed to investigate if somatic nerves travel along the entire length of the prostate, or if branches join the NVB distally. In addition, we sought to describe the location of nerves with respect to the NVB and their position around the prostate (anterior to posterior).

MATERIALS AND METHODS

Specimen Identification

After receiving institutional ethics approval, archived formalin-fixed, paraffin-embedded RP tissue was retrieved for analysis.

Specimens from patients who underwent RP with wide local excision of the periprostatic soft tissue were considered for inclusion. Patients with prior pelvic radiation, surgery, or trauma were excluded due to the risk of disruption of normal anatomy.

A specialist pathologist performed a preliminary review of hematoxylin and eosin (H&E)-stained slides from all potentially relevant cases to ensure that the specimens contained NVB tissue prior to inclusion. Ultimately, hemiprostates from 6 RP specimens were included for analysis.

During routine processing for clinical evaluation, formalin-fixed RP specimens are inked over the surface; the dimensions and weight are recorded and the specimens are then cut into blocks following a standard protocol, comprising parasagittal sections of the apex and base at approximately 10 mm depth and intervening transverse sections (perpendicular to the prostatic urethra). All of these sections are approximately 5 mm thick. All included cases had representative sections taken from the base, midzone, and apex of the prostate for examination. Due to the technique of tissue block preparation, the number of sections available for analysis varied (between 4 and 5) depending upon the prostate size. 4 μm sections of tissue were cut from each representative block and mounted on standard glass microscopy slides for staining and immunohistochemistry.

Histological Staining

No specific marker for somatic nerves exists. Previous histological studies have used myelination as a surrogate marker for the identification of somatic nerves.[11] However, as both somatic and preganglionic parasympathetic nerves are myelinated, markers of myelination alone are insufficient to isolate somatic fibers. Therefore, a 2-step process was employed. Representative slides from included specimens were stained with Masson's trichrome (MT), which stains myelin a brilliant red-orange.[11] Parasympathetic nerves were identified using an antibody directed against neuronal nitric oxide synthase (nNOS), which is present in the peripheral parasympathetic nerves that innervate the cavernous body and cavernosal arteries.[16] The antibody used was a rabbit monoclonal antibody, anti-nNOS (neuronal) antibody (Abcam, ab76067; Sapphire Bioscience Pty Ltd. Waterloo NSW). The antibody was diluted 1:500 with Leica diluent. nNOS slides were processed on Leica "BONDMAX" using Bond polymer refine detection kit with epitope retrieval (Epitope Retrieval Solution 1) for 20 minutes. Somatic fibers were isolated by identifying myelinated nerves that were nNOS negative.

All stains and immunohistochemistry were also tested on control tissue (anal sphincter) (Supplementary Fig. S1).

Slide Analysis

Slides were scanned using a 40× objective (400× equivalent magnification) with the Aperio whole slide scanner (Aperio Scanscope XT). Digital analysis was undertaken using Aperio ImageScope viewing software (Leica Biosystems Imaging Inc, Vista, CA). Nerves were identified and annotated (according to nerve type) on each slide by the primary investigator and cross-checked by a specialist pathologist. Nerve cross-sectional area was calculated using the digital volume calculator on the ImageScope software.

Nerve location was described with reference to 6 equal sectors (numbered 1 to 6 from anterior to posterior) around the hemiprostate (Supplementary Fig. S2). This was based on previous studies in this area.[17] The sector was recorded against the level of the tissue block being analyzed (apex, midzone, or base).

Three-dimensional reconstruction was performed using Reconstruct software (Neural Systems Laboratory, Boston University)[18] to give a visual representation of the nerve distribution.

Statistical Analysis

Descriptive statistics (count, percentage, mean, and standard deviation) were used to describe periprostatic nerve distribution. In the case of sectors that had significant missing tissue (which precluded analysis), results were not imputed. When greater than 3 tissue sections were available, the most apical and basal blocks were used to represent the apex and base, and results from intervening blocks were combined to obtain an average (mean) midzone result for each hemiprostate.

RESULTS

Six hemiprostates were stained with MT and anti-nNOS (Supplementary Fig. S3). In total, 1412 nerve bundles were identified at the base and 851 at the apex. Overall, 2015 nerve bundles were identified in the intervening midzone tissue sections. After the results from cases that had multiple midzone sections had been combined and averaged to obtain a mean midzone result per hemiprostate, the total number of nerves for analysis in the midzone was 949.

The mean hemiprostate nerve count declined from 235 at the base, to 158 in the midzone and 142 at the apex (Table 1). Similarly, the mean cross-sectional nerve volume decreased from 3.41 mm^2 at the base to 1.51 mm^2 at the apex (Supplementary Table S1).

The proportion of somatic nerves accounted for less than 5% of the total number of nerves at the prostate base, midzone, and apex when measured either by nerve count or cross-sectional neural area (Table 1 and Supplementary Table S1). The vast majority of nerves identified at each

Table 1. Hemiprostate periprostatic nerve count at the base, midzone, and apex

Sector	Myelinated		Nonmyelinated	Ganglion	Total
	Somatic	+nNOS			
Base					
No. identified (% total nerves at base)	35 (2.5)	27 (1.9)	1287 (91.2)	63 (4.5)	1412 (100)
Mean nerve count ± SD	5.83 ± 3.66	4.5 ± 3.02	214.5 ± 123.09	10.5 ± 4.93	235.33 ± 128.55
Midzone					
No. identified (% total nerves at midzone)	32 (3.3)	16 (1.7)	857 (90.3)	45 (4.8)	949 (100)
Mean nerve count ± SD	5.25 ± 4.24	2.61 ± 2.30	142.78 ± 62.33	7.53 ± 2.94	158.17 ± 64.12
Apex					
No. identified (% total nerves at apex)	22 (2.6)	47 (5.5)	765 (89.9)	17 (2.0)	851 (100)
Mean nerve count ± SD	3.67 ± 4.32	7.83 ± 10.28	127.5 ± 37.96	2.83 ± 2.64	141.83 ± 39.92

nNOS, neuronal nitric oxide synthase; SD, standard deviation.

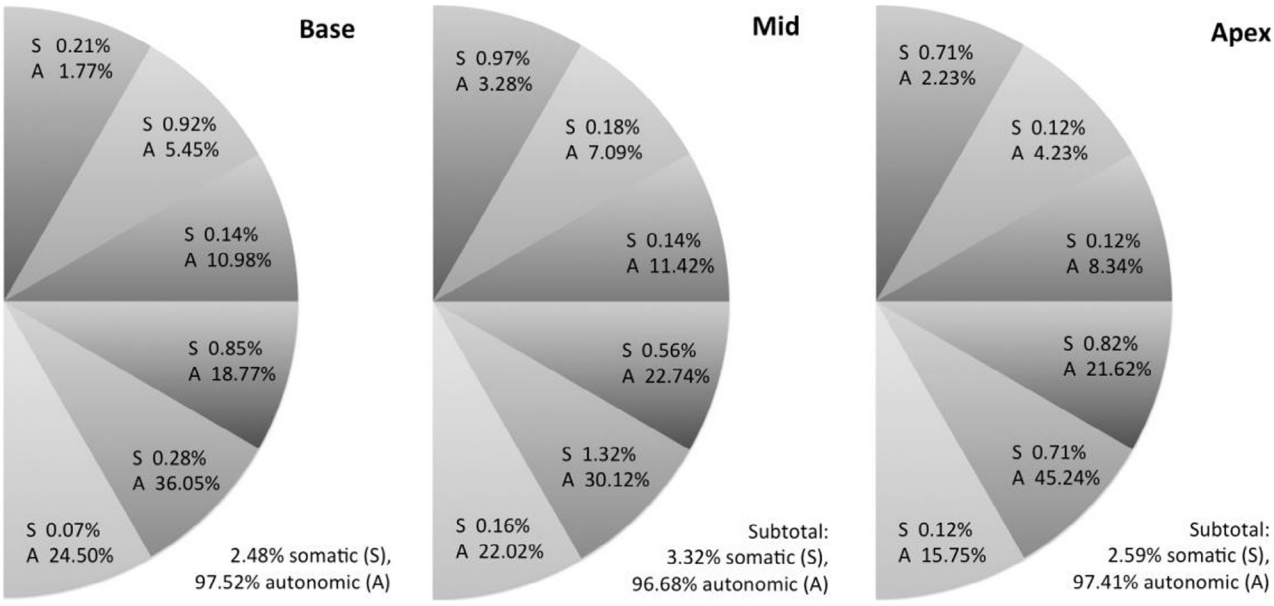

Figure 1. Proportion of somatic and autonomic nerves per sector at the base, midzone, and apex of the prostate.

level were nonmyelinated (approximately 90%). Although there was a slight decrease in the mean somatic nerve count from base to apex (5.83 to 3.67), the proportion of somatic nerves was relatively constant at each level (between 2.5% and 3.3%) due to a relative decrease in all nerve subtypes toward the apex.

With reference to the sector distribution of somatic vs autonomic nerves at each level (Fig. 1), the autonomic nerves were distributed mainly between sectors 3 to 6 at the base, and then became more concentrated in sectors 4 and 5 toward the apex. This corresponds to the autonomic neurovascular bundle. Only a small proportion of autonomic fibers were identified anteriorly in sectors 1 and 2. The somatic nerves in each sector comprised between 0.07% and 1.32% of the total nerve count at each level of the prostate (Fig. 1). Analysis of the distribution of somatic nerves by sector, with reference to the total number of periprostatic somatic nerves, revealed that the somatic nerves were most likely to be located in the anterior (sectors 1 and 2) and posterolateral areas (sectors 4 and 5) (Fig. 2). Overall, 20.5% of all somatic nerves were in sector 1, 17.7% were in sector 2, 27.5% were in sector 4, and 25.4% were in sector 5.

The location of somatic nerves in relation to the prostatic capsule was variable. In some instances, somatic nerves were located immediately adjacent to the prostatic capsule, and in other cases they were located further out into the periprostatic fat or were within the neurovascular bundle tissue.

Three-dimensional reconstruction of an illustrative case of periprostatic nerve distribution (Fig. 3) provides visual representation of the typical distribution of periprostatic nerves observed in this study.

DISCUSSION

This study has demonstrated that somatic nerves are present in the periprostatic tissue at the level of the prostate base, midzone, and apex. These somatic fibers comprise a small

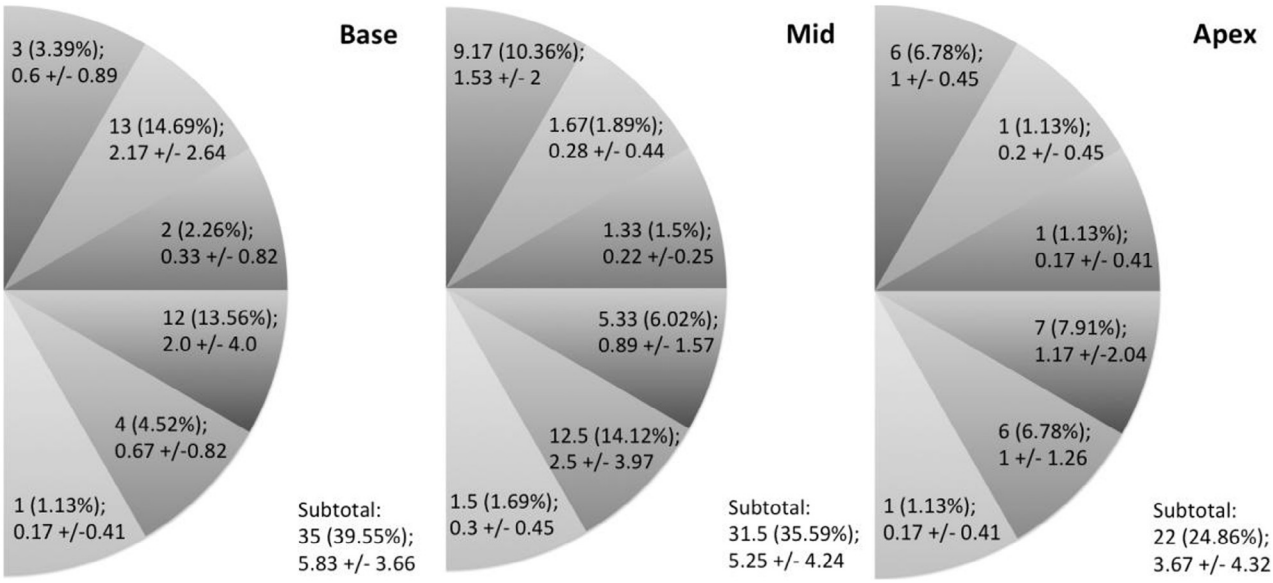

Figure 2. Distribution of somatic nerves: total number of somatic nerves counted per sector for 6 hemiprostates (% total periprostatic somatic fibers); mean ± SD per sector (per hemiprostate).

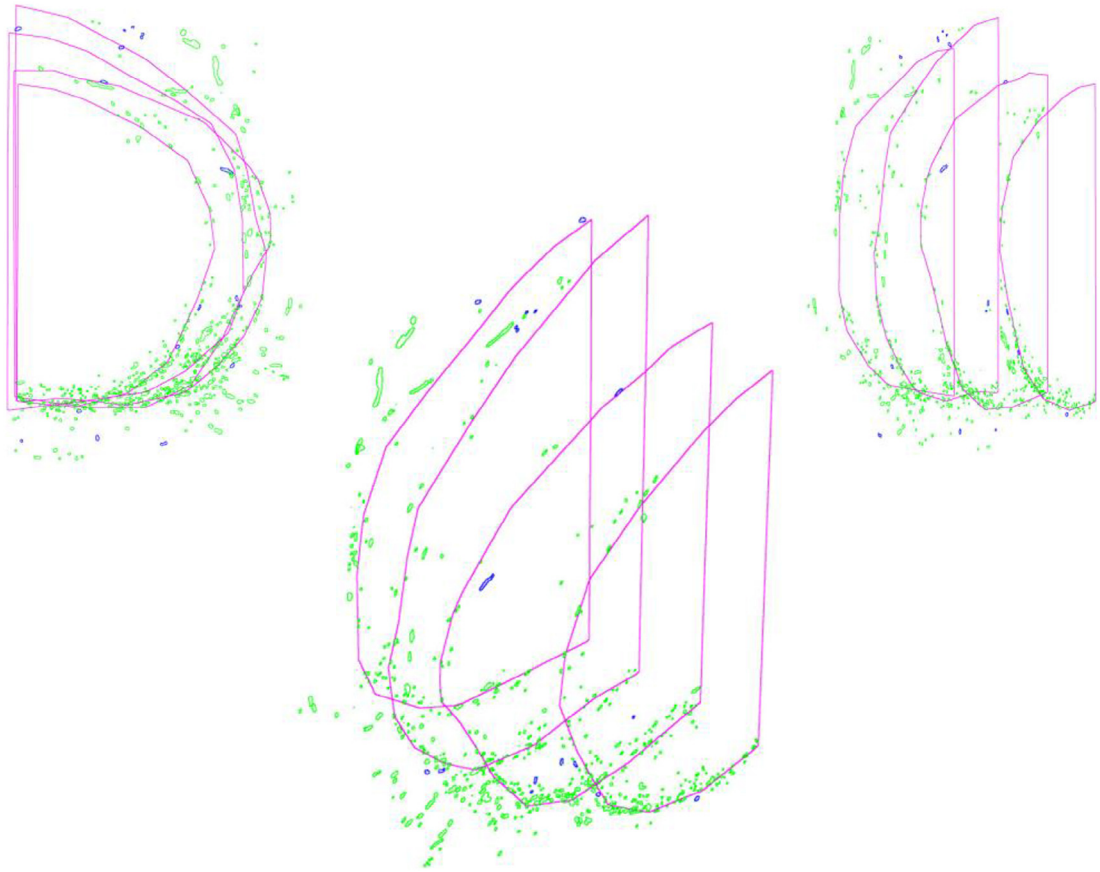

Figure 3. Three-dimensional reconstruction of periprostatic nerve distribution; somatic nerves (blue), autonomic nerves (green). (Color version available online.)

proportion of all periprostatic nerves, and tend to be located anteriorly (sectors 1 and 2) or in the posterolateral neurovascular bundle region (sectors 4 and 5). There was no increase in the number of somatic nerves from base to apex to suggest that somatic fibers converge on the prostate distally. In fact, there was a decrease in the mean somatic nerve count toward the prostatic apex. This may represent the termination of some somatic fibers supplying the levator

ani muscle, or may be attributed to the varying margins of periprostatic tissue on the surgical specimens at each level.

The main strength of this study is the precision with which somatic nerves were identified. This is the first study that we are aware of, to use whole slide scanning with 40× objective to identify periprostatic nerves. Digital annotation also facilitated accurate analysis of both number and cross-sectional area of nerves and provided a platform for three-dimensional reconstruction. Also, by using both MT (to identify myelination) and nNOS (to exclude parasympathetic myelinated nerves), this study has demonstrated that a significant proportion of periprostatic myelinated nerves are in fact parasympathetic in nature (approximately one to two thirds). Therefore, the use of myelination alone as a means to identify somatic nerves is inaccurate and overestimates the number of somatic nerves. In our study, somatic fibers were identified as MT positive and nNOS negative; false-negative nNOS staining could further overestimate the proportion of somatic nerves. Previous studies investigating urological neuroanatomy have used myelination as a surrogate marker for somatic fibers either without taking into consideration the presence of myelinated preganglionic parasympathetic nerves[8] or without taking specific measures to distinguish somatic and autonomic nerves.[11]

Few histological studies exist that directly address our research question of the presence and distribution of periprostatic somatic nerves. Our group previously evaluated the specific distribution (and proportion) of somatic fibers in the periprostatic region.[13] In that study, somatic nerves were present in the periprosatic tissue from base to apex at a much higher proportion than in the present investigation, accounting for 18%, 16.5%, and 15.5% of the total nerve fibers identified at the level of the base, midzone, and apex, respectively. However, that study was designed to characterize sympathetic and parasympathetic nerves, thus somatic nerves were identified on H&E staining and no targeted staining was undertaken to specifically isolate somatic fibers. Furthermore, analysis of stained slides and counting of nerve fibers were done by hand and overall numbers of nerves identified (per specimen) were significantly fewer than what was identified in our study despite the use of cadaveric tissue, which presumably included a wider margin of periprostatic tissue than was available in the surgical specimens utilized in the current study. Similarly, in a study by Clarebrough et al, periprostatic mean nerve count and cross-sectional neural area from H&E-stained slides of 13 cadaveric hemiprostates yielded significantly fewer nerves and smaller cross-sectional area than in our study.[17] Clarebrough et al's results came from digital analyses at 20× objective. A proportion of small nerves may not have been appreciated in these studies due to the lower power of magnification used for analysis. The high nerve counts in our study may be reassuring that the surgical radical prostatectomy specimens evaluated contained sufficient periprostatic tissue for evaluation.

The methods used in our study (analysis at high-power magnification, and use of dual staining to improve the specificity of somatic nerve identification) have helped clarify our understanding of the actual number and proportion of periprostatic somatic nerves.

Limitations

One of the challenges of histological studies of neuroanatomy is the absence of any specific marker that allows the precise identification of somatic motor nerves. The technique employed in this study enabled the isolation of somatic myelinated nerves from preganglionic parasympathetic myelinated nerves. However, it was not possible to determine if these somatic fibers were motor or sensory in nature.

Another limitation of this study is the relatively small sample size. Although the number of individuals included is small, nerve measurements were consistent across patients, suggesting that the point estimates are reasonable. While all specimens were from patients with known prostate cancer, this is clinically relevant as this represents the men who undergo radical prostatectomy.

CONCLUSION

A small proportion of periprostatic nerves are somatic in nature. These fibers are evident from the base to the apex of the prostate and are at risk of injury during radical prostatectomy. Further research is required to clarify the course and function of these nerves.

References

1. Boorjian SA, Eastham JA, Graefen M, et al. A critical analysis of the long-term impact of radical prostatectomy on cancer control and function outcomes. *Eur Urol.* 2012;61:664-675.
2. Ficarra V, Novara G, Ahlering TE, et al. Systematic review and meta-analysis of studies reporting potency rates after robot-assisted radical prostatectomy. *Eur Urol.* 2012;62:418-430.
3. Ficarra V, Novara G, Rosen RC, et al. Systematic review and meta-analysis of studies reporting urinary continence recovery after robot-assisted radical prostatectomy. *Eur Urol.* 2012;62:405-417.
4. Groutz A, Blaivas JG, Chaikin DC, et al. The pathophysiology of post-radical prostatectomy incontinence: a clinical and video urodynamic study. *J Urol.* 2000;163:1767-1770.
5. Majoros A, Bach D, Keszthelyi A, et al. Urinary incontinence and voiding dysfunction after radical retropubic prostatectomy (prospective urodynamic study). *Neurourol Urodyn.* 2006;25:2-7.
6. Strasser H, Klima G, Poisel S, et al. Anatomy and innervation of the rhabdosphincter of the male urethra. *Prostate.* 1996;28:24-31.
7. Song LJ, Lu HK, Wang JP, et al. Cadaveric study of nerves supplying the membranous urethra. *Neurourol Urodyn.* 2010;29:592-595.
8. Narayan P, Konety B, Aslam K, et al. Neuroanatomy of the external urethral sphincter: implications for urinary continence preservation during radical prostate surgery. *J Urol.* 1995;153:337-341.
9. Shafik A, Doss S. Surgical anatomy of the somatic terminal innervation to the anal and urethral sphincters: role in anal and urethral surgery. *J Urol.* 1999;161:85-89.
10. Akita K, Sakamoto H, Sato T. Origins and courses of the nervous branches to the male urethral sphincter. *Surg Radiol Anat.* 2003;25:387-392.
11. Hollabaugh J, Robert S, Dmochowski RR, Steiner MS. Neuroanatomy of the male rhabdosphincter. *Urology.* 1997;49:426-434.
12. Zvara P, Carrier S, Kour N-W, et al. The detailed neuroanatomy of the human striated urethral sphincter. *Br J Urol.* 1994;74:182-187.

13. Costello AJ, Dowdle BW, Namdarian B, et al. Immunohistochemical study of the cavernous nerves in the periprostatic region. *BJU Int*. 2011;107:1210-1215.
14. Ganzer R, Stolzenburg J-U, Wieland WF, et al. Anatomic study of periprostatic nerve distribution: immunohistochemical differentiation of parasympathetic and sympathetic nerve fibres. *Eur Urol*. 2012;62:1150-1156.
15. Reeves F, Preece P, Kapoor J, et al. Preservation of the neurovascular bundles is associated with improved time to continence after radical prostatectomy but not long-term continence rates: results of a systematic review and meta-analysis. *Eur Urol*. 2015;68:692-704.
16. Stanarius A, Ückert S, Machtens SA, et al. Immunocytochemical distribution of nitric oxide synthase in the human corpus cavernosum: an electron microscopical study using the tyramide signal amplification technique. *Urol Res*. 2001;29:168-172.
17. Clarebrough EE, Challacombe BJ, Briggs C, et al. Cadaveric analysis of periprostatic nerve distribution: an anatomical basis for high anterior release during radical prostatectomy? *J Urol*. 2011;185:1519-1525.
18. Fiala JC. Reconstruct: a free editor for serial section microscopy. *J Microsc*. 2005;218:52-61.

APPENDIX

Supplementary Data

Supplementary data associated with this article can be found, in the online version, at http://dx.doi.org/10.1016/j.urology.2016.08.027.